

# Deterministic generation of photonic entangled states using decoherence-free subspaces

Oriol Rubies-Bigorda,<sup>1,2,\*</sup> Stuart J. Masson,<sup>3</sup> Susanne F. Yelin,<sup>2</sup> and Ana Asenjo-Garcia<sup>3</sup>

<sup>1</sup>*Physics Department, Massachusetts Institute of Technology, Cambridge, Massachusetts 02139, USA*

<sup>2</sup>*Department of Physics, Harvard University, Cambridge, Massachusetts 02138, USA*

<sup>3</sup>*Department of Physics, Columbia University, New York, New York 10027, USA*

We propose the use of collective states of matter as a resource for the deterministic generation of quantum states of light, which are fundamental for quantum information technologies. Our minimal model consists of three emitters coupled to a half-waveguide, i.e., a one-dimensional waveguide terminated by a mirror. Photon-mediated interactions between the emitters result in the emergence of bright and dark states. The dark states form a decoherence-free subspace, protected from dissipation. Local driving of the emitters and control of their resonance frequencies allows to perform arbitrary quantum gates within the decoherence-free subspace. Coupling to bright states facilitates photon emission, thereby enabling the realization of quantum gates between light and matter. We demonstrate that sequential application of these gates leads to the generation of photonic entangled states, such as Greenberger-Horne-Zeilinger and one- and two-dimensional cluster states.

Large entangled states are a crucial resource in quantum technologies such as quantum computation, metrology and sensing [1–5], yet they are typically hard to create. A prominent example of multipartite entanglement is provided by Greenberger–Horne–Zeilinger (GHZ) states [6, 7], useful for quantum metrology [8], where qubits exist in a superposition of either all in one state or all in the other. Another relevant class of entangled states is the multi-dimensional cluster states [9–11], where qubits are arranged in a lattice and entangled with their nearest neighbors. Two-dimensional (2D) cluster states are particularly significant, as they constitute a universal resource for measurement-based quantum computation [9, 11, 12].

Entanglement between photons can be generated deterministically by interfacing light with a multilevel quantum emitter [13, 14]. During the last decades, numerous protocols have been developed to sequentially emit entangled photons. For example, it has been theoretically proposed to couple a quantum emitter to a cavity [15], as well as to a one-dimensional (1D) photonic channel [16] to generate 1D cluster states. This latter idea has been generalized to 2D cluster states by means of time-delayed feedback loops in chiral waveguides [17]. Other suggested platforms include arrays of single emitters coupled to waveguides [18–20], and an ancillary atom interacting with sets of atomic arrays in free space [21, 22]. The realization of more general tensor network states has also been proposed [23, 24]. Experimental implementations of these protocols have followed recently. For instance, few-photon GHZ and linear cluster states have been generated with a quantum dot [25], a superconducting qubit [26] and a neutral atom [27]. The generation of a 2D cluster state with microwave photons has been recently reported, by coupling superconducting qubits to waveguides [20, 28]. In all these works, the entangling gates between light and matter harness the multilevel structure of a single emitter.

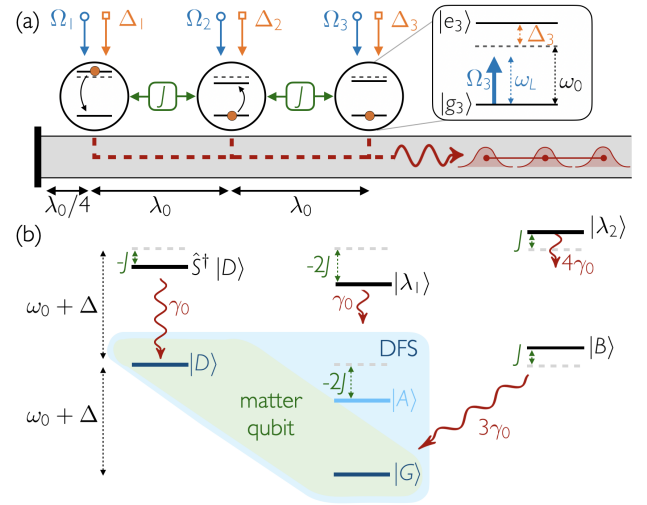


Figure 1. Local operations together with long-range interactions between three emitters coupled to a half-waveguide result in the generation of entangled photons. (a) Proposed setup: external fields allow for tunable and local frequency shifts  $\Delta_{1,3} = \Delta$  and  $\Delta_2 = \Delta + \delta$  and Rabi frequencies  $\Omega_n$  (orange and blue control lines, respectively). Coherent exchange interactions  $J$  between neighboring emitters (depicted in green) can be engineered via external couplers. (b) Collective basis states in the absence of drive and for  $\delta = -J$ . The ground state  $|G\rangle$  and the two single-excitation states  $|D\rangle$  and  $|A\rangle$  are dark and form a decoherence-free subspace (DFS).  $|G\rangle$  and  $|D\rangle$  form the matter qubit that remains entangled with the emitted photons, whereas  $|A\rangle$  is used as an auxiliary state for conditional photon emission. The remaining states are bright (decay is shown in red).

Light-matter interactions are more efficient when multiple emitters are involved due to interference [29–33]. In particular, in the presence of a shared dielectric environment, the electromagnetic vacuum mediates long-range interactions between emitters, modifying their radiative properties [34–37]. This can lead to the emergence of a

decoherence-free subspace (DFS) [38–41], which consists of a set of “dark” states that are decoupled from the (electromagnetic) environment and therefore also from dissipation. Prior theoretical works have shown that multiple “collective” qubits can be encoded within this subspace, and have devised protocols for universal quantum computation by realizing gates between the states in the DFS [42–44]. Interactions between emitters also result in the emergence of “bright” states. By coupling the DFS to bright states, it is possible to emit few-photon pulses [45, 46].

In this manuscript, we propose to generate entangled states of light by harnessing the collective basis spanned by just a few two-level systems. A minimal configuration of three emitters coupled to a waveguide terminated by a mirror gives rise to a qutrit in the decoherence-free subspace. By means of local frequency shifts and weak driving fields, we attain a full set of logical quantum gates for the qutrit. Further control over the coupling between (collective) dark and bright states via local frequency shifts enables the emission of photons with arbitrary temporal profiles, as well as the design of entangling quantum gates between the matter qutrit and the photonic qubits. Sequential application of these quantum gates on the emitters results in the generation of photonic entangled states. We exemplify the procedure by theoretically demonstrating the preparation of GHZ, 1D and 2D cluster states. Our protocol can be implemented in state-of-the-art transmon devices [20, 28, 31, 37, 47].

*System.*— Our minimal setup consists of three two-level emitters [48] with transition frequency  $\omega_0$  coupled to a one-dimensional waveguide terminated by a mirror, i.e., a half-waveguide, as shown in Fig. 1(a). The emitters are located at distances  $x_n = (n + 1/4)\lambda_0$  from the mirror, where  $\lambda_0 = 2\pi c/\omega_0$ . The half-waveguide ensures that light is emitted into a single direction. This is in contrast to the traditional waveguide setup (i.e., without a mirror) where photons are emitted in both directions, requiring strong chirality [47] or the recombination of both pulses [49] to enforce a single output channel.

Provided that the propagation time of a photon between the emitters is much smaller than their characteristic timescale, the photonic degrees of freedom of the waveguide can be traced out under the Born-Markov approximation [50, 51]. This leads to an effective master equation for the reduced density matrix of the emitters,  $\dot{\hat{\rho}} = -i[\hat{H}, \hat{\rho}] + \mathcal{L}[\hat{\rho}]$  (setting  $\hbar = 1$ ). For the specific locations of the emitters along the half-waveguide, the waveguide-mediated coherent interaction is zero and the Lindbladian reduces to [50, 51]

$$\mathcal{L}[\hat{\rho}] = 3\gamma_0 \left( \hat{S}\hat{\rho}\hat{S}^\dagger - \frac{1}{2}\{\hat{S}^\dagger\hat{S}, \hat{\rho}\} \right), \quad (1)$$

where  $\gamma_0$  is the single-emitter decay rate. Photon emission corresponds to the action of the collective jump operator  $\hat{S} = \sum_{n=1}^3 \hat{\sigma}_n/\sqrt{3}$ , where  $\hat{\sigma}_n = |g_n\rangle\langle e_n|$  are lowering

operators, and occurs at a rate three times larger than that of a single emitter.

The coherent evolution of the system is governed by the Hamiltonian

$$\hat{H} = \Delta \sum_n \hat{\sigma}_n^\dagger \hat{\sigma}_n + \delta \hat{\sigma}_2^\dagger \hat{\sigma}_2 + J \left( \hat{\sigma}_1^\dagger \hat{\sigma}_2 + \hat{\sigma}_2^\dagger \hat{\sigma}_3 + h.c. \right) + \sum_n \left( \Omega_n e^{-i(\omega_L - \omega_0)t} \hat{\sigma}_n^\dagger + h.c. \right). \quad (2)$$

Here, the first and third emitters are shifted by  $\Delta$  from the bare transition frequency  $\omega_0$ , whereas the second emitter acquires a shift  $\Delta + \delta$  [orange control lines in Fig. 1(a)]. Additionally, neighboring emitters undergo coherent exchange interactions at a rate  $J$ , which can be engineered via external couplers [37, 47]. Finally, we consider the emitters to be driven at a frequency  $\omega_L$  via control lines or fields external to the half-waveguide that allow for position-dependent Rabi frequencies  $\Omega_n$  with arbitrary relative phases [37]. All parameters  $\Delta$ ,  $\delta$ ,  $J$  and  $\Omega_n$  can be varied over time.

Collective dissipation leads to the emergence of states that are decoupled from decay or dissipation, i.e., that are in the null space of  $\hat{S}$ . This decoherence-free subspace [41, 44] is spanned by the ground state  $|G\rangle \equiv |ggg\rangle$  and the single-excitation collective states  $|D\rangle = (|egg\rangle - |gge\rangle)/\sqrt{2}$  and  $|A\rangle = (|egg\rangle - 2|geg\rangle + |gge\rangle)/\sqrt{6}$ . The remaining single-excitation state  $|B\rangle = (|egg\rangle + |geg\rangle + |gge\rangle)/\sqrt{3}$  is bright and decays to the ground state at a rate  $3\gamma_0$ , while the three states containing two excitations are bright and decay with rates ranging from  $\gamma_0$  to  $4\gamma_0$ . The fully excited state,  $|eee\rangle$ , is also bright, with a decay rate  $3\gamma_0$ . For  $\delta = -J$  and in the absence of drive (i.e.,  $\Omega_n = 0$ ), the ground and single-excitation states are also eigenstates of the Hamiltonian in Eq. (2). In particular,  $|D\rangle$ ,  $|B\rangle$  and  $|A\rangle$  acquire frequency shifts  $\Delta$ ,  $\Delta + J$  and  $\Delta - 2J$  respectively, while the states in the two-excitation manifold are shifted by  $2\Delta \pm J$  and  $2\Delta - 2J$ , as illustrated in Fig. 1(b) and discussed in the Supplemental Material (SM [52]). Frequency shifts  $\delta \neq -J$  lead to a coherent coupling between the single-excitation states  $|A\rangle$  and  $|B\rangle$ , while  $|D\rangle$  remains an eigenstate of the system.

Prior proposals to prepare time-binned entangled states of photons rely on a single multi-level quantum emitter with two long-lived states forming a matter qubit, from which conditional photon emission (i.e., a CNOT gate) is possible [16, 17, 26, 28]. In our proposal, instead, the necessary level structure is provided by the collective states of the three-emitter system. The two long-lived states that comprise the matter qubit are chosen as  $|D\rangle$  and  $|G\rangle$ . Additional coupling to the auxiliary dark state  $|A\rangle$  and the bright states gives rise to controlled interactions between light and matter. In what follows, we demonstrate full control over the quantum state of the emitters within the DFS, and further show that the coupling to bright states allows to engineer the entangling light-matter CNOT and CZ gates. Sequential application

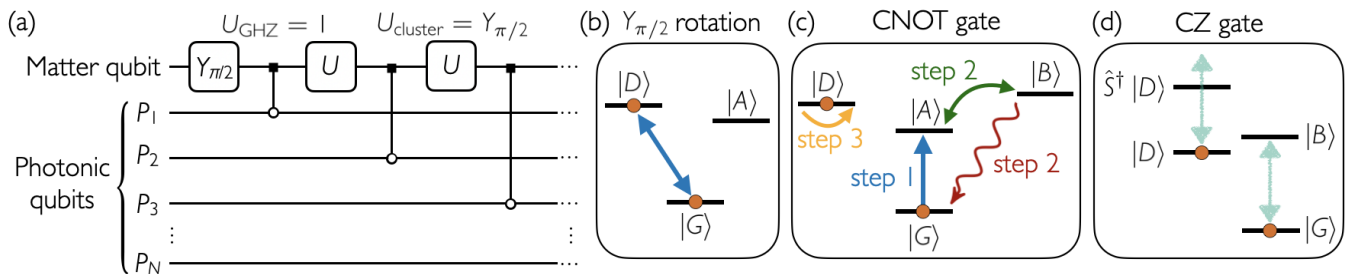


Figure 2. Gate protocol for the generation of entangled photon states. (a) Schematics of the quantum circuit. The matter qubit and photonic qubits are initialized in the ground state. The emission of each entangled photonic qubit is achieved through the sequential operation of a light-matter CNOT gate (i.e., emission of a photon conditional on the state of the matter qubit) followed by a unitary operation  $U$  on the matter qubit. To generate GHZ states,  $U \equiv \mathcal{I}$ , and to generate one-dimensional cluster states,  $U \equiv Y_{\pi/2}$  (i.e., a  $\pi/2$ -rotation around the  $y$  axis). (b-d) Implementation of the quantum gates in the collective basis. (b) The  $Y_{\pi/2}$  rotation of the matter qubit is attained by driving the  $|D\rangle \leftrightarrow |G\rangle$  transition. Population of higher excited states is suppressed due to the large off-resonance shift  $J$  and decay rate  $\gamma_0$  of the bright two-excitation states. (c) The CNOT gate or conditional photon emission is attained in two steps. First, the amplitude in  $|G\rangle$  is transferred to the auxiliary dark state  $|A\rangle$ . Then, a nonzero detuning  $\delta \neq -J$  is applied to the second emitter, thereby coupling  $|A\rangle$  and  $|B\rangle$  and leading to the emission of a photon with arbitrary wavepacket. Finally, a phase gate is applied to compensate the phase acquired by  $|D\rangle$  during the first two steps. (d) The controlled phase gate is realized by scattering a photonic qubit from the collective system, in the low-excitation limit. For large coherent coupling  $J$ , the photon is resonant with  $|G\rangle \leftrightarrow |B\rangle$  but far off-resonant with  $|D\rangle \leftrightarrow \hat{S}^\dagger |D\rangle$ , and consequently acquires different phases depending on the state of matter qubit.

of matter and light-matter gates [as shown in Fig. 2(a)] yields the generation of entangled photon states. The full protocol to produce GHZ and cluster states is described below.

*Matter gates in the DFS.*— Arbitrary quantum operations on the DFS-encoded qutrit state  $|\psi_{DFS}\rangle = d(t)e^{-i\omega_0 t}|D\rangle + g(t)|G\rangle + a(t)e^{-i\omega_0 t}|A\rangle$  can be realized via rotations between two pairs of states  $\{|G\rangle, |D\rangle, |A\rangle\}$  together with independent control over their phases [53–55]. The implementation of high-fidelity quantum gates requires the applied control sequences to not populate the bright states outside the DFS. This is naturally the case in the absence of drive and provided that  $\delta = -J$  [see level diagram in Fig. 1(b)]. Driving fields, on the other hand, can result in transitions to the bright collective states in higher excitation manifolds. However, if the timescales associated to the decay from the bright states are much faster than the average time it takes for the drive to excite them (i.e.,  $\Omega \ll \gamma_0$ ), the bright states are only virtually populated and the dynamics of the system is effectively projected into the DFS due to the quantum Zeno effect. This constraint on the Rabi frequency thus limits the speed of the gates. Nevertheless, the addition of external couplers allows for stronger drives and significantly faster gate times, as excitation is prevented by photon blockade when  $\Omega \ll J$ . The constraint on gate time thus becomes  $T \sim \Omega^{-1} \gg 1/\sqrt{\gamma_0^2 + J^2}$ , which can be reduced by increasing  $\gamma_0$  and  $J$ .

Arbitrary rotations between  $|G\rangle$  and  $|D\rangle$  require the collective system to be driven on resonance ( $\omega_L = \omega_0$  and  $\Delta = 0$ ) with the profile of  $|D\rangle$ , i.e.,  $\Omega_1 = -\Omega_3 = \Omega e^{i\phi}/\sqrt{2}$  and  $\Omega_2 = 0$ , as illustrated in Fig. 2(b). The primary source of error is additional coupling of  $|D\rangle$  to

the bright two-excitation states  $S^\dagger |A\rangle$  and  $S^\dagger |B\rangle$ , which are off-resonant by at least  $J$ , as well as coupling of  $|A\rangle$  to  $S^\dagger |D\rangle$ , which is off-resonant by  $J$ . As shown in the SM, for  $\Omega^2 \ll \gamma_0^2 + J^2$ , the dynamics of the system after a time  $T = \theta/\Omega$  implements (up to small corrections) the quantum gate

$$\mathcal{R}_{DG}(\theta, \phi, \chi) = \begin{pmatrix} \cos(\theta) & -ie^{i\phi} \sin(\theta) & 0 \\ -ie^{-i\phi} \sin(\theta) & \cos(\theta) & 0 \\ 0 & 0 & e^{i\chi} \end{pmatrix}, \quad (3)$$

in the basis  $\{|D\rangle, |G\rangle, |A\rangle\}$  and for  $\chi = 2JT$ . Notably,  $\mathcal{R}_{DG}(\pi/4, -\pi/2, \chi) \equiv Y_{\pi/2}$  corresponds to the  $\pi/2$ -rotation around the  $y$  axis of the Bloch sphere of the matter qubit. Similarly, arbitrary rotations between the dark states  $|G\rangle$  and  $|A\rangle$ , defined by the rotation matrix

$$\mathcal{R}_{GA}(\theta, \phi, \chi) = \begin{pmatrix} e^{-i\chi} & 0 & 0 \\ 0 & \cos(\theta) & -ie^{i\phi} \sin(\theta) \\ 0 & -ie^{-i\phi} \sin(\theta) & \cos(\theta) \end{pmatrix}, \quad (4)$$

are obtained by matching the drive profile to the profile of  $|A\rangle$ ,  $\Omega_1 = -\Omega_2/2 = \Omega_3 = \Omega e^{i\phi}/\sqrt{6}$ . The phase acquired by  $|D\rangle$  during the operation is  $\chi = -2JT$  (see SM).

Arbitrary phase control requires three phase gates. First, coherent coupling in the absence of drives (i.e.,  $J = -\delta \neq 0$  and  $\Omega_n = \Delta = 0$ ) gives rise to a phase for state  $|A\rangle$  of  $-2JT$ . Conversely, applying only an equal detuning to all qubits (i.e.,  $\Delta \neq 0$  and  $\Omega_n = J = \delta = 0$ ) results in equal phases acquired by  $|D\rangle$  and  $|A\rangle$  of  $\phi = \Delta T$ . Control over the phase of  $|G\rangle$  requires drive of the form  $\Omega_n = \Omega/\sqrt{3}$ , which couples off-resonantly every state in the DFS to a higher-excited state, introducing different Stark shifts to each state. With these

three phase gates, it becomes possible to produce arbitrary phase rotations within the DFS (see SM for details). Since the detuning  $\Delta$ , the drive detuning  $\omega_0 - \omega_L$ , and the coherent external coupling  $J$  can typically be much larger than  $\gamma_0$ , the phase gates can be performed in a time  $T \ll \gamma_0^{-1}$ .

*Light-matter gates.*— Generation of entangled photonic states requires entangling gates between the DFS and the photonic qubits. A CNOT or conditional emission gate can be implemented in three steps, as illustrated in Fig. 2(c). First, we apply a rotation  $\mathcal{R}_{GA}$  that transfers the amplitude in the ground state  $|G\rangle$  to the auxiliary dark state  $|A\rangle$ , i. e.,  $d_0 |D\rangle + g_0 |G\rangle \rightarrow d_0 e^{i\chi} |D\rangle - i g_0 |A\rangle$ . Then, a non-zero detuning  $\delta \neq -J$  is applied to the second emitter, which couples  $|A\rangle$  and  $|B\rangle$  while  $|D\rangle$  remains an eigenstate of the Hamiltonian. This effectively leads to the emission of a photon in the  $k$ -th step only if the system is in  $|A\rangle$ , resulting in the state  $d_0 e^{i\chi'} |D\rangle \otimes |0_k\rangle + g_0 |G\rangle \otimes |1_k\rangle$ . Finally, the phase  $\chi'$  acquired by  $|D\rangle$  during both operations is compensated by applying a phase gate. Notably, arbitrary temporal wavepackets for the emitted photons are attained by appropriately controlling  $\delta(t)$  during the emission process (see SM).

A CZ or conditional phase gate is implemented by interfacing again a previously-created photonic qubit with the system of emitters. More precisely, the incoming photon couples the states  $|G\rangle$  and  $|B\rangle$ , as well as  $|D\rangle$  and  $\hat{S}^\dagger |D\rangle$ . Notably, the frequencies associated to both transitions differ by  $2J$ , resulting in the photon acquiring different phases depending on the state of the matter qubit [see Fig. 2(d)]. A photon with a small bandwidth (i. e., a large temporal width) and that is resonant with the  $|G\rangle \leftrightarrow |B\rangle$  transition will acquire a phase flip when scattering from  $|G\rangle$ . If the matter qubit is in  $|D\rangle$ , however, a far off-resonant photon ( $J \gg \gamma_0$ ) does not acquire any phase upon scattering, i. e.,  $\phi_D = \pi + 2 \arctan(4J/\gamma_0) \rightarrow 0$  (see SM). That is, we attain a CZ gate under which only the state with one photon and the matter qubit in  $|G\rangle$  changes sign.

Finally, the collective level structure of the system allows to disentangle the emitters from the photonic states in a simple manner. This is achieved by slightly modifying the CNOT gate applied to generate the last photonic qubit. In particular, one needs to apply a  $\pi$ -rotation that transfers  $|D\rangle$  to  $|G\rangle$ ,  $Y_\pi \equiv \mathcal{R}_{DG}(\pi/2, -\pi/2, \chi)$ , between the transfer  $|G\rangle \rightarrow |A\rangle$  and the photon emission process. Then, the collective system finishes the protocol in the ground state  $|G\rangle$  while the last photonic qubit is still emitted in an entangled fashion.

*Generating GHZ and cluster states.*— Sequential application of rotations on the matter qubit and the light-matter CNOT gate results in a train of entangled photonic qubits in different time bins. An  $m$ -qubit photonic GHZ state is obtained by repeatedly applying the CNOT gate  $m$  times on the initial state  $(|G\rangle + |D\rangle)/\sqrt{2}$  and fi-

nally disentangling the matter and photons.

Similarly, an  $m$ -qubit 1D cluster state is obtained by repeatedly applying a  $\pi/2$ -rotation on the matter qubit ( $Y_{\pi/2}$ ) followed by a CNOT gate  $m$  times each. Following the proposal in Ref. [17], higher-dimensional entanglement structures can be generated by letting the  $k$ -th photonic qubit interact with the system of emitters a second time between the emission of photon  $k + N - 1$  and  $k + N$ . A two-dimensional photonic cluster state in an  $M \times N$  lattice (where  $MN$  is the total number of emitted photons) is obtained if the matter qubit applies the controlled phase gate  $CZ$  on the  $k$ -th photon. For that, the emitted photons are reflected back to the system of emitters by an additional switchable mirror (e. g., an additional emitter) placed at the transmitting end of the half-waveguide [28]. The transmission line needs to be long enough such that it can support  $N$  temporally non-overlapping photons and, consequently, emission or scattering processes of the emitter system and the switchable mirror are independent.

*Timescales and errors.*— Up to this point, gates have been assumed to be ideal. In practice, however, these gates may accumulate errors arising from (i) small populations of the bright states outside the DFS, (ii) independent photon emission at a rate  $\gamma'$  into modes different than those of the half-waveguide and described by the Lindbladian  $\sum_{n=1}^3 \gamma' (\hat{\sigma}_n \hat{\rho} \hat{\sigma}_n^\dagger - \{\hat{\sigma}_n^\dagger \hat{\sigma}_n\}/2)$ , or (iii) imperfect control of the Hamiltonian (i. e., of the detunings, the drives and the coherent interaction). Figure 3(a) and (b) shows the error or infidelity  $\epsilon = 1 - \mathcal{F}$  for the  $Y_{\pi/2}$  rotation (orange) and the amplitude transfer from  $|G\rangle$  to  $|A\rangle$  of the CNOT gate (blue). The error is analytically (see SM) and numerically found to scale as  $\epsilon \propto \gamma_0 T^{-1} (J^2 + \gamma_0^2)^{-1}$ . Optimal gate fidelities are thus achieved for large coherent couplings  $J$ , as dynamics are better constrained to the DFS and lost population in the two-excitation bright states decreases. Similarly, longer gate times  $T$  are associated with smaller drive strengths  $\Omega$ , and a subsequent stronger effect of the Zeno effect and the photon blockade mechanism. In the presence of emission into undesired channels, the error eventually increases for large  $T$ , thereby setting an optimal gate time.

The infidelity of the CZ gate under ideal conditions (i. e., zero photon bandwidth) scales as  $\propto \gamma_0^2/J^2$ , as shown in the inset of Fig. 3(c) and demonstrated in the SM. For photonic wavepackets with finite bandwidth  $\mathcal{B}$ , different frequency components acquire slightly different phases during the scattering process associated to the CZ gate. This leads to a reduction of the fidelity with increasing bandwidth, as shown in Fig. 3(c). For photons obtained by setting a constant coupling between  $|A\rangle$  and  $|B\rangle$  during the photon emission process, the infidelity for small bandwidths scales as  $\mathcal{B}/\gamma_0$ . The infidelity can be substantially reduced by shaping the wavepacket. For Gaussian wavepackets, for example, the infidelity scales as  $\sim \mathcal{B}^2/\gamma_0^2$ .

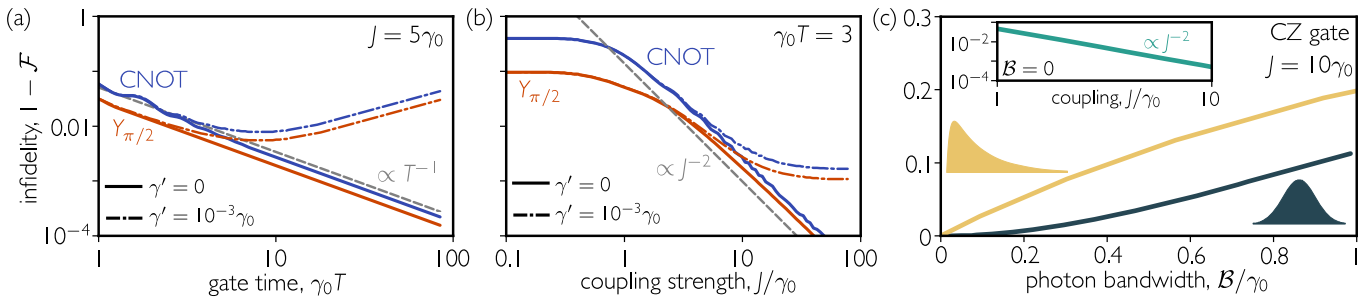


Figure 3. Gate infidelity  $\epsilon = 1 - \mathcal{F}$ . (a,b) Infidelity of the CNOT gate (blue) and the  $Y_{\pi/2}$  rotation (orange) as a function of (a) gate time  $T$  and (b) strength of the coherent coupling  $J$ . In the absence of emission into undesired channels,  $\gamma' = 0$ , the infidelity scales as  $\epsilon \propto \gamma_0 J^{-2} T^{-1}$  for  $J \gg \gamma_0$  (see grey dashed lines as a reference). For  $\gamma' \neq 0$ , the infidelity increases for long gate times and saturates for large coherent couplings. (c) Infidelity of the CZ gate as a function of the photon bandwidth  $\mathcal{B}$  at  $J = 10\gamma_0$ . We consider a Gaussian photon (dark green) and a photon obtained by setting a constant coupling between  $|A\rangle$  and  $|B\rangle$  during the emission process (yellow). The inset shows the infidelity of the CZ gate for an ideal photon with zero bandwidth as a function of the coupling strength  $J$ .

*Implementation.*— Our protocols for photonic entangled-state generation can be implemented in various platforms. A particularly suited option consists of superconducting qubits [28, 31, 37, 47] coupled to a transmission line with an open end, which effectively acts as a mirror [56]. Local frequency shifts and driving fields with arbitrary phase profiles can be achieved through external control lines [37], and time-dependent coherent interactions between different qubits (with strengths up to  $J \sim 10\gamma_0$ ) can be implemented via capacitive couplers [37, 47]. While transmon qubits are not strictly two-level systems, they can exhibit anharmonicities  $\gtrsim 10^2\gamma_0$  [47], such that their multi-level structure can be neglected. Finally, they typically exhibit dissipative couplings to the waveguide that are orders of magnitude larger than their dephasing or non-radiative decay rates, a crucial requirement to generate high-fidelity entangled states with a large number of photonic qubits. Alternative implementations include atoms or quantum dots coupled to nanophotonic waveguides [29, 35, 57] or (“bad”) cavities with one partially-reflecting mirror. In this case, direct addressing of dark states could be achieved via free-space driving fields, while the coherent exchange coupling  $J$  can be engineered via Rydberg interactions [58].

*Conclusions and outlook.*— We have demonstrated that logical quantum gates can be performed between collective dark states of two-level emitters coupled to a common radiation field. Together with coupling to collective bright states, this results in controlled light-matter gates that can be leveraged to generate photonic entangled states, such as GHZ and cluster states. Fast operations are attained by introducing large coherent exchange interactions, and the protocol duration is limited by the time required to emit the photonic qubits. Photon emission could be accelerated by leveraging superradiance, which becomes more prominent in larger arrays.

Our protocol could be generalized to realize other types of entanglement structures, such as tensor network states [24, 59]. Alternatively, systems containing four or more qubits exhibit dark states with at least two excitations [51], which could be used to create higher-dimensional photonic states [60, 61] where the photonic qubits are replaced by qudits (encoded in Fock states with different photon number). Beyond the generation of quantum states of light, collective dark states and their selective coupling to radiating states can also be leveraged as quantum memories [33, 36, 62], facilitating communication and networking between distant nodes [63–65].

*Acknowledgements.*— O.R.B. acknowledges support from Fundación Mauricio y Carlota Botton and from Fundació Bancaria “la Caixa” (LCF/BQ/AA18/11680093). We acknowledge additional support by the National Science Foundation through the CAREER Award (No. 2047380) and the QII-TAQS program (No. 1936345), the Air Force Office of Scientific Research through their Young Investigator Prize (No. 21RT0751), as well as by the David and Lucile Packard Foundation. SFY acknowledges funding by the NSF through the CUA PFC (PHY-2317134) and through PHY-2207972.

\* orubies@mit.edu

- [1] L. K. Grover, Quantum mechanics helps in searching for a needle in a haystack, *Phys. Rev. Lett.* **79**, 325 (1997).
- [2] R. Horodecki, P. Horodecki, M. Horodecki, and K. Horodecki, Quantum entanglement, *Rev. Mod. Phys.* **81**, 865 (2009).
- [3] C. H. Bennett, Quantum information, *Phys. Scr.* **1998**, 210 (1998).
- [4] V. Giovannetti, S. Lloyd, and L. Maccone, Quantum metrology, *Phys. Rev. Lett.* **96**, 010401 (2006).

- [5] N. Gisin and R. Thew, Quantum communication, *Nat. Photonics* **1**, 165 (2007).
- [6] D. M. Greenberger, M. A. Horne, and A. Zeilinger, Going beyond bell's theorem, in *Bell's Theorem, Quantum Theory and Conceptions of the Universe*, edited by M. Kafatos (Springer Netherlands, Dordrecht, 1989) pp. 69–72.
- [7] N. D. Mermin, Extreme quantum entanglement in a superposition of macroscopically distinct states, *Phys. Rev. Lett.* **65**, 1838 (1990).
- [8] J. J. . Bollinger, W. M. Itano, D. J. Wineland, and D. J. Heinzen, Optimal frequency measurements with maximally correlated states, *Phys. Rev. A* **54**, R4649 (1996).
- [9] R. Raussendorf and H. J. Briegel, A one-way quantum computer, *Phys. Rev. Lett.* **86**, 5188 (2001).
- [10] H. J. Briegel and R. Raussendorf, Persistent entanglement in arrays of interacting particles, *Phys. Rev. Lett.* **86**, 910 (2001).
- [11] H. J. Briegel, D. E. Browne, W. Dür, R. Raussendorf, and M. Van den Nest, Measurement-based quantum computation, *Nat. Phys.* **5**, 19 (2009).
- [12] R. Raussendorf, D. E. Browne, and H. J. Briegel, Measurement-based quantum computation on cluster states, *Phys. Rev. A* **68**, 022312 (2003).
- [13] L.-M. Duan and H. J. Kimble, Scalable photonic quantum computation through cavity-assisted interactions, *Phys. Rev. Lett.* **92**, 127902 (2004).
- [14] K. Koshino, S. Ishizaka, and Y. Nakamura, Deterministic photon-photon  $\sqrt{\text{swap}}$ gate using a  $\Lambda$  system, *Phys. Rev. A* **82**, 010301 (2010).
- [15] C. Schön, E. Solano, F. Verstraete, J. I. Cirac, and M. M. Wolf, Sequential generation of entangled multi-qubit states, *Phys. Rev. Lett.* **95**, 110503 (2005).
- [16] N. H. Lindner and T. Rudolph, Proposal for pulsed on-demand sources of photonic cluster state strings, *Phys. Rev. Lett.* **103**, 113602 (2009).
- [17] H. Pichler, S. Choi, P. Zoller, and M. D. Lukin, Universal photonic quantum computation via time-delayed feedback, *PNAS* **114**, 11362 (2017).
- [18] S. E. Economou, N. Lindner, and T. Rudolph, Optically generated 2-dimensional photonic cluster state from coupled quantum dots, *Phys. Rev. Lett.* **105**, 093601 (2010).
- [19] A. Russo, E. Barnes, and S. E. Economou, Generation of arbitrary all-photonic graph states from quantum emitters, *New J. Phys.* **21**, 055002 (2019).
- [20] J. O'Sullivan, K. Reuer, A. Grigorev, X. Dai, A. Hernández-Antón, M. H. Muñoz-Arias, C. Hellings, A. Flasby, D. C. Zanuz, J.-C. Besse, A. Blais, D. Malz, C. Eichler, and A. Wallraff, *Deterministic generation of a 20-qubit two-dimensional photonic cluster state* (2024), [arXiv:2409.06623 \[quant-ph\]](https://arxiv.org/abs/2409.06623).
- [21] R. Bekenstein, I. Pikovski, H. Pichler, E. Shahmoon, S. F. Yelin, and M. D. Lukin, Quantum metasurfaces with atom arrays, *Nat. Phys.* **16**, 676 (2020).
- [22] Z.-Y. Wei, D. Malz, A. González-Tudela, and J. I. Cirac, Generation of photonic matrix product states with Rydberg atomic arrays, *Phys. Rev. Res.* **3**, 023021 (2021).
- [23] S. Xu and S. Fan, Generate tensor network state by sequential single-photon scattering in waveguide QED systems, *APL Photonics* **3**, 116102 (2018).
- [24] Z.-Y. Wei, D. Malz, and J. I. Cirac, Sequential generation of projected entangled-pair states, *Phys. Rev. Lett.* **128**, 010607 (2022).
- [25] I. Schwartz, D. Cogan, E. R. Schmidgall, Y. Don, L. Gantz, O. Kenneth, N. H. Lindner, and D. Gershoni, Deterministic generation of a cluster state of entangled photons, *Science* **354**, 434 (2016).
- [26] J.-C. Besse, K. Reuer, M. C. Collodo, A. Wulff, L. Wernli, A. Copetudo, D. Malz, P. Magnard, A. Akin, M. Gabureac, G. J. Norris, J. I. Cirac, A. Wallraff, and C. Eichler, Realizing a deterministic source of multipartite-entangled photonic qubits, *Nat. Commun.* **11**, 4877 (2020).
- [27] P. Thomas, L. Ruscio, O. Morin, and G. Rempe, Efficient generation of entangled multiphoton graph states from a single atom, *Nature* **608**, 677 (2022).
- [28] V. S. Ferreira, G. Kim, A. Butler, H. Pichler, and O. Painter, Deterministic generation of multidimensional photonic cluster states with a single quantum emitter, *Nat. Phys.* **20**, 865 (2024).
- [29] A. Goban, C.-L. Hung, S.-P. Yu, J. D. Hood, J. A. Muniz, J. H. Lee, M. J. Martin, A. C. McClung, K. S. Choi, D. E. Chang, O. Painter, and H. J. Kimble, Atom–light interactions in photonic crystals, *Nat. Commun.* **5**, 3808 (2014).
- [30] E. Shahmoon, D. S. Wild, M. D. Lukin, and S. F. Yelin, Cooperative resonances in light scattering from two-dimensional atomic arrays, *Phys. Rev. Lett.* **118**, 113601 (2017).
- [31] M. Mirhosseini, E. Kim, X. Zhang, A. Sipahigil, P. B. Dieterle, A. J. Keller, A. Asenjo-Garcia, D. E. Chang, and O. Painter, Cavity quantum electrodynamics with atom-like mirrors, *Nature* **569**, 692 (2019).
- [32] J. Rui, D. Wei, A. Rubio-Abadal, S. Hollerith, J. Zeiher, D. M. Stamper-Kurn, C. Gross, and I. Bloch, A subradiant optical mirror formed by a single structured atomic layer, *Nature* **583**, 369 (2020).
- [33] O. Rubies-Bigorda, V. Walther, T. L. Patti, and S. F. Yelin, Photon control and coherent interactions via lattice dark states in atomic arrays, *Phys. Rev. Res.* **4**, 013110 (2022).
- [34] R. H. Dicke, Coherence in spontaneous radiation processes, *Phys. Rev.* **93**, 99 (1954).
- [35] A. Goban, C.-L. Hung, J. D. Hood, S.-P. Yu, J. A. Muniz, O. Painter, and H. J. Kimble, Superradiance for atoms trapped along a photonic crystal waveguide, *Phys. Rev. Lett.* **115**, 063601 (2015).
- [36] A. Asenjo-Garcia, M. Moreno-Cardoner, A. Albrecht, H. J. Kimble, and D. E. Chang, Exponential improvement in photon storage fidelities using subradiance and “selective radiance” in atomic arrays, *Phys. Rev. X* **7**, 031024 (2017).
- [37] M. Zanner, T. Orell, C. M. F. Schneider, R. Albert, S. Oleschko, M. L. Juan, M. Silveri, and G. Kirchmair, Coherent control of a multi-qubit dark state in waveguide quantum electrodynamics, *Nat. Phys.* **18**, 538 (2022).
- [38] P. Zanardi and M. Rasetti, Noiseless quantum codes, *Phys. Rev. Lett.* **79**, 3306 (1997).
- [39] P. Facchi and S. Pascazio, Quantum Zeno subspaces, *Phys. Rev. Lett.* **89**, 080401 (2002).
- [40] D. A. Lidar and B. K. Whaley, Decoherence-free subspaces and subsystems, in *Irreversible Quantum Dynamics*, edited by F. Benatti and R. Floreanini (Springer Berlin Heidelberg, Berlin, Heidelberg, 2003) pp. 83–120.
- [41] A. Beige, D. Braun, and P. L. Knight, Driving atoms into decoherence-free states, *New J. Phys.* **2**, 22 (2000).
- [42] D. A. Lidar, I. L. Chuang, and K. B. Whaley, Decoherence-free subspaces for quantum computation,

- Phys. Rev. Lett.* **81**, 2594 (1998).
- [43] A. Beige, D. Braun, B. Tregenna, and P. L. Knight, Quantum computing using dissipation to remain in a decoherence-free subspace, *Phys. Rev. Lett.* **85**, 1762 (2000).
- [44] V. Paulisch, H. J. Kimble, and A. González-Tudela, Universal quantum computation in waveguide QED using decoherence free subspaces, *New J. Phys.* **18**, 043041 (2016).
- [45] A. González-Tudela, V. Paulisch, H. J. Kimble, and J. I. Cirac, Efficient multiphoton generation in waveguide quantum electrodynamics, *Phys. Rev. Lett.* **118**, 213601 (2017).
- [46] A. González-Tudela, V. Paulisch, D. E. Chang, H. J. Kimble, and J. I. Cirac, Deterministic generation of arbitrary photonic states assisted by dissipation, *Phys. Rev. Lett.* **115**, 163603 (2015).
- [47] B. Kannan, A. Almanakly, Y. Sung, A. Di Paolo, D. A. Rower, J. Braumüller, A. Melville, B. M. Niedzielski, A. Karamlou, K. Serniak, A. Vepsäläinen, M. E. Schwartz, J. L. Yoder, R. Winik, J. I.-J. Wang, T. P. Orlando, S. Gustavsson, J. A. Grover, and W. D. Oliver, On-demand directional microwave photon emission using waveguide quantum electrodynamics, *Nat. Phys.* **19**, 394 (2023).
- [48] While the minimal setup described in the main text consists of three emitters, entangled photonic states can also be attained with only two emitters coupled to the half-waveguide. However, this requires a more complex control of the system, as discussed in the Supplemental Material.
- [49] V. Paulisch, M. Perarnau-Llobet, A. González-Tudela, and J. I. Cirac, Quantum metrology with one-dimensional superradiant photonic states, *Phys. Rev. A* **99**, 043807 (2019).
- [50] N. Fayard, L. Henriët, A. Asenjo-Garcia, and D. E. Chang, Many-body localization in waveguide quantum electrodynamics, *Phys. Rev. Res.* **3**, 033233 (2021).
- [51] O. Rubies-Bigorda, S. J. Masson, S. F. Yelin, and A. Asenjo-Garcia, Engineering and addressing dark states in atomic arrays coupled to a half-waveguide, in preparation.
- [52] See the Supplemental Material for a detailed derivation of the matter gates, the emission of single photons with arbitrary wavepackets and the light-matter gates, as well as their respective fidelities. The Supplemental Material also includes the description of an alternative protocol based on two emitters only.
- [53] J. Lindon, A. Tashchilina, L. W. Cooke, and L. J. LeBlanc, Complete unitary qutrit control in ultracold atoms, *Phys. Rev. Appl.* **19**, 034089 (2023).
- [54] S. Dogra, Arvind, and K. Dorai, Determining the parity of a permutation using an experimental NMR qutrit, *Phys. Lett. A* **378**, 3452 (2014).
- [55] A. B. Klimov, R. Guzmán, J. C. Retamal, and C. Saavedra, Qutrit quantum computer with trapped ions, *Phys. Rev. A* **67**, 062313 (2003).
- [56] I.-C. Hoi, A. F. Kockum, L. Tornberg, A. Pourkabirian, G. Johansson, P. Delsing, and C. M. Wilson, Probing the quantum vacuum with an artificial atom in front of a mirror, *Nat. Phys.* **11**, 1045 (2015).
- [57] A. Tiranov, V. Angelopoulos, C. J. van Diepen, B. Schirnski, O. A. D. Sandberg, Y. Wang, L. Midolo, S. Scholz, A. D. Wieck, A. Ludwig, A. S. Sørensen, and P. Lodahl, Collective super- and subradiant dynamics between distant optical quantum emitters, *Science* **379**, 389 (2023).
- [58] P. L. Ocola, I. Dimitrova, B. Grinkemeyer, E. Guardado-Sanchez, T. Đorđević, P. Samutpraphoot, V. Vuletić, and M. D. Lukin, Control and entanglement of individual Rydberg atoms near a nanoscale device, *Phys. Rev. Lett.* **132**, 113601 (2024).
- [59] F. Verstraete and J. I. Cirac, Matrix product states represent ground states faithfully, *Phys. Rev. B* **73**, 094423 (2006).
- [60] X.-M. Hu, W.-B. Xing, C. Zhang, B.-H. Liu, M. Pivovluska, M. Huber, Y.-F. Huang, C.-F. Li, and G.-C. Guo, Experimental creation of multi-photon high-dimensional layered quantum states, *npj Quantum Information* **6**, 88 (2020).
- [61] W.-B. Xing, X.-M. Hu, Y. Guo, B.-H. Liu, C.-F. Li, and G.-C. Guo, Preparation of multiphoton high-dimensional ghz states, *Opt. Express* **31**, 24887 (2023).
- [62] R. Holzinger, R. Gutiérrez-Jáuregui, T. Hönigl-Decrinis, G. Kirchmair, A. Asenjo-Garcia, and H. Ritsch, Control of localized single- and many-body dark states in waveguide QED, *Phys. Rev. Lett.* **129**, 253601 (2022).
- [63] J. I. Cirac, P. Zoller, H. J. Kimble, and H. Mabuchi, Quantum state transfer and entanglement distribution among distant nodes in a quantum network, *Phys. Rev. Lett.* **78**, 3221 (1997).
- [64] H. J. Kimble, The quantum internet, *Nature* **453**, 1023 (2008).
- [65] A. Almanakly, B. Yankelevich, M. Hays, B. Kannan, R. Assouly, A. Greene, M. Gingras, B. M. Niedzielski, H. Stickler, M. E. Schwartz, K. Serniak, J. I.-J. Wang, T. P. Orlando, S. Gustavsson, J. A. Grover, and W. D. Oliver, *Deterministic remote entanglement using a chiral quantum interconnect* (2024), arXiv:2408.05164 [quant-ph].
- [66] M. Horodecki, P. Horodecki, and R. Horodecki, General teleportation channel, singlet fraction, and quasidistillation, *Phys. Rev. A* **60**, 1888 (1999).
- [67] E. M. Fortunato, M. A. Pravia, N. Boulant, G. Teklemariam, T. F. Havel, and D. G. Cory, Design of strongly modulating pulses to implement precise effective hamiltonians for quantum information processing, *J. Chem. Phys.* **116**, 7599 (2002).
- [68] M. A. Nielsen, A simple formula for the average gate fidelity of a quantum dynamical operation, *Phys. Lett. A* **303**, 249 (2002).
- [69] G. S. Vasilev, D. Ljunggren, and A. Kuhn, Single photons made-to-measure, *New J. Phys.* **12**, 063024 (2010).
- [70] T. Utsugi, A. Goban, Y. Tokunaga, H. Goto, and T. Aoki, Gaussian-wave-packet model for single-photon generation based on cavity quantum electrodynamics under adiabatic and nonadiabatic conditions, *Phys. Rev. A* **106**, 023712 (2022).

# Deterministic generation of photonic entangled states using decoherence-free subspaces: Supplemental Material

Oriol Rubies-Bigorda<sup>1,2</sup>, Stuart J. Masson<sup>3</sup>, Susanne F. Yelin<sup>2</sup>, and Ana Asenjo-Garcia<sup>3</sup>

<sup>1</sup>*Physics Department, Massachusetts Institute of Technology, Cambridge, Massachusetts 02139, USA*

<sup>2</sup>*Department of Physics, Harvard University, Cambridge, Massachusetts 02138, USA*

<sup>3</sup>*Department of Physics, Columbia University, New York, New York 10027, USA*

## CONTENTS

I. Matter gates in the decoherence-free subspace	1
I.A. Arbitrary rotations between $ D\rangle$ and $ G\rangle$	1
I.B. Arbitrary rotations between $ G\rangle$ and $ A\rangle$	3
I.C. Phase control of $ A\rangle$	3
I.D. Phase control of $ D\rangle$	3
I.E. Phase control of $ G\rangle$	4
II. Single photon emission	4
III. Light-matter gates	5
III.A. CNOT gate	6
III.B. CZ gate	6
IV. Photonic entangled state generation with two two-level emitters coupled to a half-waveguide	8

## I. MATTER GATES IN THE DECOHERENCE-FREE SUBSPACE

In this section, we present in detail the full set of quantum gates between the three dark states in the decoherence-free subspace (DFS), namely the ground state  $|G\rangle \equiv |ggg\rangle$  and the single-excitation collective states  $|D\rangle = (|egg\rangle - |gge\rangle)/\sqrt{2}$  and  $|A\rangle = (|egg\rangle - 2|geg\rangle + |gge\rangle)/\sqrt{6}$ . We consider the Hamiltonian in Eq. (2) of the main text with  $\delta = -J$ . In terms of the lowering and rising operators associated to the collective states,  $\hat{\sigma}_B = (\hat{\sigma}_1 + \hat{\sigma}_2 + \hat{\sigma}_3)/\sqrt{3} \equiv \hat{S}$ ,  $\hat{\sigma}_D = (\hat{\sigma}_1 - \hat{\sigma}_3)/\sqrt{2}$  and  $\hat{\sigma}_A = (\hat{\sigma}_1 - 2\hat{\sigma}_2 + \hat{\sigma}_3)/\sqrt{6}$ , it can be expressed as

$$\hat{H}_{nH} = \left( \Delta + J - i\frac{3\gamma_0}{2} \right) \hat{\sigma}_B^\dagger \hat{\sigma}_B + \Delta \hat{\sigma}_D^\dagger \hat{\sigma}_D + (\Delta - 2J) \hat{\sigma}_A^\dagger \hat{\sigma}_A + \sum_{k \in \{D, A, B\}} \left( \Omega_k e^{-i(\omega_L - \omega_0)t} \hat{\sigma}_k^\dagger + h.c. \right), \quad (\text{S1})$$

where the non-Hermitian term  $-i3\gamma_0\hat{\sigma}_B^\dagger\hat{\sigma}_B/2$  describes the decay of atomic excitation via photon emission into the half-waveguide. In the absence of drive and as shown in Fig. 1(b), the single-excitation eigenstates of the non-Hermitian Hamiltonian  $\hat{H}_{nH}$  are  $|B\rangle = \hat{\sigma}_B^\dagger|G\rangle$  (shifted from  $\omega_0$  by  $\Delta + J$  and exhibiting a decay rate  $3\gamma_0$ ),  $|D\rangle$  (shifted by  $\Delta$ ) and  $|A\rangle$  (shifted by  $\Delta - 2J$ ). The two-excitation eigenstates are  $|S_D\rangle$  (shifted from  $2\omega_0$  by  $2\Delta - J$  and exhibiting a decay rate  $\gamma_0$ ),  $|\lambda_1\rangle = \epsilon_1|S_B\rangle + \epsilon_2|S_A\rangle$  (shifted by  $2\Delta - 2J$  and exhibiting a decay rate  $\approx \gamma_0$ ) and  $|\lambda_2\rangle = \epsilon_2|S_B\rangle - \epsilon_1|S_A\rangle$  (shifted by  $2\Delta + J$  and exhibiting a decay rate  $\approx 4\gamma_0$ ). Here, we have defined the states  $|S_k\rangle = \hat{S}^\dagger|k\rangle/||\hat{S}^\dagger|k\rangle||$  for  $k \in \{D, A, B\}$ . For the sake of brevity, we refrain from writing down the explicit form of  $\epsilon_{1,2}$ . Finally, the drive introduces couplings between states with different excitation numbers.

Arbitrary single-qutrit gates for a general state  $|\psi_{DFS}(t)\rangle = d(t)e^{-i\omega_0 t}|D\rangle + g(t)|G\rangle + a(t)e^{-i\omega_0 t}|A\rangle$  in the DFS can be obtained by sequentially applying the following five operations, which enable arbitrary phase control and arbitrary rotations between two pairs of states [S53–S55].

### I.A. Arbitrary rotations between $|D\rangle$ and $|G\rangle$

We drive the  $|G\rangle \leftrightarrow |D\rangle$  transition on resonance,  $\omega_0 = \omega_L$  and  $\Delta = 0$ , by applying  $\Omega_D = \Omega e^{i\phi}$  and  $\Omega_B = \Omega_A = 0$ . For the individual emitters, this corresponds to the drive  $\Omega_1 = -\Omega_3 = \Omega e^{i\phi}/\sqrt{2}$ . This drive does not only couple  $|D\rangle$  and  $|G\rangle$  with strength  $\Omega$ , but also gives rise to the transitions  $|A\rangle \leftrightarrow |S_D\rangle$  and  $|D\rangle \leftrightarrow |\lambda_{1,2}\rangle$ . Notably, the first process is off-resonant by  $-J$ , whereas the latter are off-resonant by  $-2J$  and  $J$ . Additionally, the two-excitation bright states



decay at rates ranging from  $\gamma_0$  to  $4\gamma_0$ . For weak drive compared to the combined effect of the off-resonance and decay rates,  $\Omega^2 \ll \gamma_0^2 + J^2$ , the bright states outside the DFS can be adiabatically eliminated. To leading order in the small parameter  $\Omega^2/(\gamma_0^2 + J^2)$ , they project the state back into the DFS, resulting in the Hamiltonian

$$\hat{H}_{DG} \approx -2J |A\rangle \langle A| + \Omega e^{i\phi} |D\rangle \langle G| + \Omega e^{-i\phi} |G\rangle \langle D|, \quad (\text{S2})$$

where we have only included the terms involving the three dark states. After a time  $T \sim \Omega^{-1} \gg 1/\sqrt{J^2 + \gamma_0^2}$ , these dynamics generate the arbitrary rotations  $\mathcal{R}_{DG}$  given by Eq. (3) in the main text.

In reality, the coupling to the bright states induces small errors or corrections to  $\mathcal{R}_{DG}$ . To estimate this error, we note that the protocols for entangled photon generation only involve rotations between  $|D\rangle$  and  $|G\rangle$  when there is no amplitude in  $|A\rangle$ , that is, when the initial state reads  $|\psi_{DFS}(t=0)\rangle = d_0 |D\rangle + g_0 |G\rangle$ . The evolution of the state of the system including the two-excitation states  $|\lambda_{1,2}\rangle$ , i.e.,  $|\psi(t)\rangle = d(t) |D\rangle e^{-i\omega_0 t} + g_0 |G\rangle + \lambda_1 e^{-2i\omega_0 t} |\lambda_1\rangle + \lambda_2 e^{-2i\omega_0 t} |\lambda_2\rangle$ , reads

$$\dot{g}(t) = -i\Omega e^{-i\phi} d(t), \quad (\text{S3a})$$

$$\dot{d}(t) = -i\Omega e^{i\phi} g(t) - i\Omega e^{-i\phi} \xi_1^* \lambda_1(t) - i\Omega e^{-i\phi} \xi_2^* \lambda_2(t), \quad (\text{S3b})$$

$$\dot{\lambda}_1(t) = -i(-2J - i\frac{\gamma_0}{2})\lambda_1(t) - i\Omega e^{i\phi} \xi_1 d(t), \quad (\text{S3c})$$

$$\dot{\lambda}_2(t) = -i(J - i\frac{4\gamma_0}{2})\lambda_2(t) - i\Omega e^{i\phi} \xi_2 d(t), \quad (\text{S3d})$$

where the overlaps  $\xi_{1,2} = \langle \lambda_{1,2} | \sigma_d^\dagger | D \rangle$  take values  $|\xi_{1,2}|^2 \in \{0.67, 0.33\}$  with  $|\xi_1|^2 + |\xi_2|^2 = 1$  that depend on  $J$  and  $\gamma_0$ . Note that we have assumed that the states  $|\lambda_{1,2}\rangle$  do not decay to  $|B\rangle$  and  $|A\rangle$ , but rather to states outside of the system. While this results in a lower bound for the achievable fidelities, it results in the correct scaling with the relevant system parameters, i.e.,  $J$ ,  $\gamma_0$  and the gate time  $T$ . For  $\Omega \ll \sqrt{J^2 + \gamma_0^2}$ , the rapidly evolving two-excitation bright states can be adiabatically eliminated by setting  $d\lambda_{1,2}/dt = 0$ . Solving for the instantaneous values of  $\lambda_{1,2}(t)$  as a function of  $d(t)$ , we finally obtain the effective equation for the amplitude in the dark state  $|D\rangle$ ,

$$\dot{d}(t) = -i\left(\delta_d - i\frac{\gamma_d}{2}\right) d(t) - i\Omega e^{i\phi} g(t), \quad (\text{S4})$$

where the energy shift  $\delta_d$  and decay rate  $\gamma_d$  induced by the coupling to the two-excitation states are

$$\gamma_d = \Omega^2 \gamma_0 \left( \frac{|\xi_1|^2}{4J^2 + \gamma_0^2/4} + \frac{4|\xi_2|^2}{J^2 + 4\gamma_0^2} \right), \quad \delta_d = \Omega^2 J \left( \frac{2|\xi_1|^2}{4J^2 + \gamma_0^2/4} - \frac{|\xi_2|^2}{J^2 + 4\gamma_0^2} \right). \quad (\text{S5})$$

Applying a global detuning  $\Delta = -\delta_d$  such that the drive is still on resonance with the  $|G\rangle \leftrightarrow |D\rangle$  transition and taking  $\phi = -\pi/2$ , an initial state  $|\psi(0)\rangle = d_0 |D\rangle + g_0 |G\rangle$  performs a rotation around the  $y$  axis of the qubit defined by  $|D\rangle$  and  $|G\rangle$

$$\begin{pmatrix} d(t) \\ g(t) \end{pmatrix} = \tilde{U}(t) \begin{pmatrix} d_0 \\ g_0 \end{pmatrix} = e^{-\gamma_d t/4} \begin{pmatrix} \cos(\Omega_{\text{eff}} t) - \frac{\gamma_d}{4\Omega_{\text{eff}}} \sin(\Omega_{\text{eff}} t) & -\frac{\Omega}{\Omega_{\text{eff}}} \sin(\Omega_{\text{eff}} t) \\ \frac{\Omega}{\Omega_{\text{eff}}} \sin(\Omega_{\text{eff}} t) & \cos(\Omega_{\text{eff}} t) + \frac{\gamma_d}{4\Omega_{\text{eff}}} \sin(\Omega_{\text{eff}} t) \end{pmatrix} \begin{pmatrix} d_0 \\ g_0 \end{pmatrix}, \quad (\text{S6})$$

where we have defined the effective Rabi frequency  $\Omega_{\text{eff}} = \sqrt{\Omega^2 - \gamma_d^2/16}$ . For  $\Omega_{\text{eff}} T = \pi/4$ , the evolution  $|\psi(T)\rangle = d(T)e^{-i\omega_0 T} |D\rangle + g(T) |G\rangle$  approximately results in a  $\pi/2$  rotation around the  $y$  axis, characterized by the unitary

$$\tilde{U}(T) = \frac{e^{-\gamma_d T/4}}{2} \begin{pmatrix} 1 - \frac{\gamma_d}{4\Omega_{\text{eff}}} & -\frac{\Omega}{\Omega_{\text{eff}}} \\ \frac{\Omega}{\Omega_{\text{eff}}} & 1 + \frac{\gamma_d}{4\Omega_{\text{eff}}} \end{pmatrix}, \quad (\text{S7})$$

The ideal unitary  $U$ , achieved in the case where  $\gamma_d = 0$  and thus  $\Omega_{\text{eff}} = \Omega$ , reads

$$U(T) = \frac{e^{-\gamma_d T/4}}{2} \begin{pmatrix} 1 & -1 \\ 1 & 1 \end{pmatrix}. \quad (\text{S8})$$

The average gate fidelity can be computed as [S66–S68]

$$\mathcal{F} = \frac{1 + d^{-1} |\text{tr}(U^\dagger \tilde{U})|^2}{d + 1}, \quad (\text{S9})$$

where  $d = 2$  describes the dimension of the Hilbert space. To lowest order in the small parameter  $\gamma_d/\Omega$ , the fidelity is found to be

$$\mathcal{F} = 1 - \frac{\pi\gamma_d}{12\Omega} + \mathcal{O}\left(\frac{\gamma_d^2}{\Omega^2}\right). \quad (\text{S10})$$

Noting that  $T \approx \pi/4\Omega$  and  $\gamma_d \propto \Omega^2\gamma_0/(J^2 + \gamma_0^2)$ , one readily finds that the error of the quantum gate scales as

$$\epsilon = 1 - \mathcal{F} \sim \mathcal{C} \frac{1}{T} \frac{\gamma_0}{J^2 + \gamma_0^2}, \quad (\text{S11})$$

where  $\mathcal{C}$  is a constant. We thus find that the error for  $J \gg \gamma_0$  scales as  $\epsilon \propto \gamma_0/TJ^2$ .

### I.B. Arbitrary rotations between $|G\rangle$ and $|A\rangle$

We drive the  $|G\rangle \leftrightarrow |A\rangle$  transition on resonance,  $\omega_0 = \omega_L$  and  $\Delta = 2J$ , by applying  $\Omega_A = \Omega e^{i\phi}$  and  $\Omega_B = \Omega_D = 0$ . For the individual emitters, this corresponds to the drive  $\Omega_1 = -\Omega_2/2 = \Omega_3 = \Omega e^{i\phi}/\sqrt{6}$ . Apart from coupling  $|G\rangle$  and  $|A\rangle$  with strength  $\Omega$ , this drive also gives rise to the transitions  $|D\rangle \leftrightarrow |S_D\rangle$  and  $|A\rangle \leftrightarrow |\lambda_{1,2}\rangle$ . The first process is off-resonant by  $-J$ , while the latter are off-resonant by  $-2J$  and  $-5J$ . Again, the off-resonant drive and the decay of the bright states projects the evolution of the system into the DFS for small drives  $\Omega^2 \ll \gamma_0^2 + J^2$ . To leading order, the relevant terms in the Hamiltonian read

$$\hat{H}_{GA} \approx 2J |D\rangle \langle D| + \Omega e^{i\phi} |G\rangle \langle A| + \Omega e^{-i\phi} |A\rangle \langle G|, \quad (\text{S12})$$

After a time  $T \sim \Omega^{-1} \gg 1/\sqrt{J^2 + \gamma_0^2}$ ,  $\hat{H}_{GA}$  results in the gate  $\mathcal{R}_{GA}$  given by Eq. (4), which implements arbitrary rotations between  $|G\rangle$  and  $|A\rangle$  while  $|D\rangle$  acquires a phase  $-2JT$ . The protocols for entangled state generation rely on applying  $\mathcal{R}_{GA}$  on the initial state  $|\psi(0)\rangle = d_0 |D\rangle + g_0 |G\rangle$ . As a result, the gates act on the whole DFS of dimension  $d = 3$ . Following a similar derivation as for the rotations between  $|D\rangle$  and  $|G\rangle$ , one finds the same scaling of the gate infidelity to leading order,  $\epsilon \propto \gamma_0/[T(J^2 + \gamma_0^2)]$ .

### I.C. Phase control of $|A\rangle$

Applying only the coherent coupling  $J$  results in the Hamiltonian  $\hat{H}_A = -2J |A\rangle \langle A|$ , where we have only showed the terms involving the three dark states. Applying  $\hat{H}_A$  for a time  $T$  results in the phase gate

$$\mathcal{P}_A(\phi) = \exp(-i\hat{H}_A T) = \begin{pmatrix} 1 & 0 & 0 \\ 0 & 1 & 0 \\ 0 & 0 & e^{i\phi} \end{pmatrix} \quad (\text{S13})$$

with  $\phi = 2JT$ . For large  $J$ ,  $\mathcal{P}_A(\phi)$  can be applied in a time  $T \ll \gamma_0^{-1}$ .

### I.D. Phase control of $|D\rangle$

Applying only an equal detuning  $\Delta$  to all emitters gives rise to the Hamiltonian  $\hat{H}_D = \Delta(|D\rangle \langle D| + |A\rangle \langle A|)$  within the DFS. The resulting phase gate is

$$\mathcal{P}_D(\phi) = \exp(-i\hat{H}_D T) = \begin{pmatrix} e^{-i\phi} & 0 & 0 \\ 0 & 1 & 0 \\ 0 & 0 & e^{-i\phi} \end{pmatrix} \quad (\text{S14})$$

with  $\phi = \Delta T$ . Together with  $\mathcal{P}_A$ , it allows to control the phase of state  $|D\rangle$ . Again,  $\mathcal{P}_D(\phi)$  can be applied in a time  $T \ll \gamma_0^{-1}$  by considering  $\Delta \gg \gamma_0$ .

### I.E. Phase control of $|G\rangle$

Control over the phase of the ground state is attained by shifting the resonance frequencies of the dark states via a far off-resonant drive with Rabi frequency  $\Omega_n = \Omega_B/\sqrt{3}$  equal for all emitters  $n \in \{1, 2, 3\}$ . For  $\Delta = J = \Omega_D = \Omega_A = 0$  and defining  $\delta\omega = \omega_L - \omega_0$ , the Hamiltonian (in the rotating frame of the drive) reads

$$\hat{H} = \left(-\delta\omega - i\frac{3\gamma_0}{2}\right) |B\rangle \langle B| + \left(-\delta\omega - i\frac{\gamma_0}{2}\right) (|D\rangle \langle D| + |A\rangle \langle A|) + \Omega_B \left(|G\rangle \langle B| + \frac{1}{\sqrt{3}} |D\rangle \langle S_D| + \frac{1}{\sqrt{3}} |A\rangle \langle S_A| + h.c.\right). \quad (\text{S15})$$

The resulting equation of motion for the amplitudes in  $|G\rangle$  and  $|B\rangle$ , for example, are  $\dot{g} = -i\Omega_B b$  and  $\dot{b} = -i\Omega_B - i(-\delta\omega - i3\gamma_0/2)b$ . For  $|\delta\omega| \gg \Omega_D, \gamma_0$ , the bright state can be adiabatically eliminated. To leading order, this results in a phase shift of the ground state,  $\dot{g} \approx -i\Omega_B^2 g/\delta\omega$ . A similar treatment results in the equations  $\dot{c} \approx -i\Omega_B^2 c/3\delta\omega$  for  $c \in \{d, a\}$ . After a time  $T$ , the corresponding phase gate thus reads

$$\mathcal{P}_G(\phi) = \begin{pmatrix} e^{-i\phi/3} & 0 & 0 \\ 0 & e^{-i\phi} & 0 \\ 0 & 0 & e^{-i\phi/3} \end{pmatrix} \quad (\text{S16})$$

with  $\phi = \Omega^2 T/\delta\omega$ . Together with  $\mathcal{P}_A$  and  $\mathcal{P}_D$ ,  $\mathcal{P}_G$  allows to control the phase of the ground state  $|G\rangle$ .

## II. SINGLE PHOTON EMISSION

In this section, we present the emission of single photons with arbitrary temporal wavepackets  $\psi_{\text{ph}}(t)$  (such that  $\int |\psi_{\text{ph}}(\tau)|^2 d\tau = 1$ ) from the single-excitation collective dark state  $|A\rangle = (|egg\rangle - 2|geg\rangle + |gge\rangle)/\sqrt{6}$ . This is achieved by coupling  $|A\rangle$  to the single-excitation bright state  $|B\rangle = (|egg\rangle + |geg\rangle + |gge\rangle)/\sqrt{3}$  via a detuning  $\delta \neq -J$  applied on the second emitter. In particular, in the absence of drives (i. e.,  $\Omega_k = 0$ ) and setting  $\Delta = -4J$  and  $\delta = 8J$ , the Hamiltonian for the states in the single-excitation manifold reads

$$\hat{H}_{\text{ph}}(t) = -4J(t) |D\rangle \langle D| - i\frac{3\gamma_0}{2} |B\rangle \langle B| - 3\sqrt{2}J(t) (|A\rangle \langle B| + |B\rangle \langle A|), \quad (\text{S17})$$

where  $J(t)$  may vary over time. Applying Schrödinger's equation, we readily find that the evolution of a general state  $|\psi(t)\rangle = d(t)e^{-i\omega_0 t} |D\rangle + a(t)e^{-i\omega_0 t} |A\rangle + b(t)e^{-i\omega_0 t} |B\rangle$  is given by

$$\dot{d}(t) = i4J(t)d(t), \quad (\text{S18a})$$

$$\dot{a}(t) = i3\sqrt{2}J(t)b(t), \quad (\text{S18b})$$

$$\dot{b}(t) = -\frac{3\gamma_0}{2}b(t) + i3\sqrt{2}J(t)a(t). \quad (\text{S18c})$$

The wavepacket of the emitted photon, i. e., the amplitude of the emitted electromagnetic field over time, only depends on the time-dependent amplitude  $b(t)$  of the bright state  $|B\rangle$ , and can be written as [S69, S70]

$$\psi_{\text{ph}}(t) = \sqrt{3\gamma_0}b(t). \quad (\text{S19})$$

Note that this equation implies that the fraction of the photon emitted per unit of time,  $|\dot{\psi}_{\text{ph}}(t)|^2$ , is equal to the population of the bright state multiplied by its decay rate,  $3\gamma_0|b(t)|^2$ , as expected. Before proceeding, we assume the initial amplitude in state  $|A\rangle$  to be imaginary. For a real coherent coupling  $J$ , Eq. (S18) enforces that  $a(t)$  remains imaginary and  $b(t)$  real during the whole evolution, thereby giving rise to a photon with a wavepacket  $\psi_{\text{ph}}(t)$  contained in the reals.

Crucially, for an initial state  $|\psi(0)\rangle = d_0 |D\rangle - i|a_0\rangle |A\rangle$  with  $|d_0|^2 + |a_0|^2 = 1$ , the emission of a photon only occurs if the system is initially in  $|A\rangle$ . As a result, time evolution under Eq. (S18) gives rise to conditional photon emission and leads to a final state

$$|\psi(T_{\text{em}})\rangle = d_0 e^{i4\int_0^{T_{\text{em}}} J(\tau)d\tau} e^{-i\omega_0 T_{\text{em}}} |D\rangle \otimes |0_{\text{ph}}\rangle + |a_0\rangle |G\rangle \otimes |1_{\text{ph}}\rangle, \quad (\text{S20})$$

where  $T_{\text{em}}$  denotes the total duration of the emission process (which is limited by the decay rate of  $|B\rangle$  into the waveguide,  $T_{\text{em}} \gtrsim \gamma_0^{-1}$ ), and  $|0_{\text{ph}}\rangle$  and  $|1_{\text{ph}}\rangle$  denote the states with zero or one photon with wavepacket  $\psi_{\text{ph}}(t)$ .

In what follows, we discuss how to engineer different temporal profiles  $\psi_{\text{ph}}(t)$  by controlling  $J(t)$ . Since  $|D\rangle$  is decoupled from the emission process, we consider for simplicity the initial state  $|\psi(0)\rangle = -i|A\rangle$ .

- (i) For constant coherent coupling  $J^2 > \gamma_0^2/32$ , the photon wavepacket is an exponentially decaying sinusoidal function

$$\psi_{\text{ph}}(t) = \frac{J\sqrt{3\gamma_0}}{\sqrt{J^2 - \gamma_0^2/32}} \sin\left(t\sqrt{18J^2 - 9\gamma_0^2/16}\right) e^{-3\gamma_0 t/4} \Theta(t), \quad (\text{S21})$$

whereas for constant  $J^2 < \gamma_0^2/32$ , the oscillations are fully damped

$$\psi_{\text{ph}}(t) = \frac{J\sqrt{3\gamma_0}}{\sqrt{\gamma_0^2/32 - J^2}} \sinh\left(t\sqrt{9\gamma_0^2/16 - 18J^2}\right) e^{-3\gamma_0 t/4} \Theta(t). \quad (\text{S22})$$

Here,  $\Theta(t)$  represents the heaviside function, i. e.,  $\Theta(t) = 1$  for  $t \geq 0$  and  $\Theta(t) = 0$  for  $t < 0$ .

- (ii) Generating an arbitrary photon wavepacket  $\psi_{\text{ph}}(t)$  requires to optimize the coherent coupling over time. This can be easily achieved by discretizing the emission process in small time steps of duration  $\delta t$  [S33], such that the atomic and photonic amplitudes in Eqs. (S18) and (S19) in the  $k$ -th step read

$$\psi_{\text{ph}}^{(k)} = \sqrt{3\gamma_0} b^{(k)}, \quad (\text{S23a})$$

$$b^{(k)} = b^{(k-1)} + \delta t \left( -\frac{3\gamma_0}{2} b^{(k-1)} - 3\sqrt{2} J^{(k-1)} \text{Im}\{a^{(k-1)}\} \right), \quad (\text{S23b})$$

$$a^{(k)} = b^{(k-1)} + i3\sqrt{2}\delta t J^{(k-1)} b^{(k-1)}, \quad (\text{S23c})$$

where we have used the fact that  $a(t)$  is imaginary for all times. From these equations, we can readily obtain the coherent coupling at step  $k-1$ ,  $J^{(k-1)}$ , that results in the desired photon wavepacket at step  $k$ ,  $\psi_{\text{ph}}^{(k)}$ ,

$$J^{(k-1)} = \frac{-1}{\text{Im}\{a^{(k-1)}\}} \left( b^{(k-1)} \left( \frac{3\gamma_0}{2} - \frac{1}{\delta t} \right) + \frac{\psi_{\text{ph}}^{(k)}}{\delta t \sqrt{3\gamma_0}} \right). \quad (\text{S24})$$

This simple protocol allows to find the control sequence  $J(t)$  that generates arbitrary photon wavepackets with large fidelity, provided that they are continuous, have zero amplitude at  $t = 0$  and that their duration  $T_{em}$  is longer than the inverse decay rate  $\sim \gamma_0^{-1}$ . We refer the reader to Ref. [S51] for a detailed discussion on specific examples and the errors associated to the photon emission process.

A simple analytic form of  $J(t)$  can be derived in the limit where the emission rate is much larger than the coupling between  $|A\rangle$  and  $|B\rangle$ ,  $J(t) \ll \gamma_0$ , for a Gaussian wavepacket

$$\psi_{\text{ph}}(t) = \frac{1}{\tau^{1/2}\pi^{1/4}} e^{-(t-t_0)^2/2\tau^2}. \quad (\text{S25})$$

In that case, the bright state can be adiabatically eliminated by setting  $db(t)/dt = 0$ . Formally integrating the resulting equation for the derivative of the amplitude in  $|A\rangle$ , one readily finds

$$\psi_{\text{ph}}(t) = \sqrt{\gamma_{\text{eff}}} e^{-\int_0^t dt' \gamma_{\text{eff}}(t')/2}, \quad (\text{S26})$$

where we have defined the effective decay rate  $\gamma_{\text{eff}}(t) = 24J(t)^2/\gamma_0$ . Comparing Eq. (S25) and Eq. (S26), one can finally obtain an analytical expression for the effective decay rate [S17]

$$\gamma_{\text{eff}}(t) = \frac{2e^{-(t-t_0)^2/\tau^2}}{\tau\sqrt{\pi}(1 - \text{erf}((t-t_0)/\tau))}, \quad (\text{S27})$$

where  $\text{erf}(x) = 2 \int_0^x ds e^{-s^2}/\sqrt{\pi}$  denotes the Gaussian error function.

### III. LIGHT-MATTER GATES

The generation of entangled states of light requires entangling gates between the matter qubit  $|\psi_M(t)\rangle = d(t)e^{-i\omega t}|D\rangle + g(t)|G\rangle$  and the photonic qubits (i. e., the absence or presence of a photon in a certain time bin). Here, we describe in detail how to attain the CNOT gate required for GHZ and cluster state generation, as well as the additional CZ gate needed to produce two-dimensional cluster states.

### III.A. CNOT gate

The CNOT gate for entangled state generation is always applied between the matter qubit and the  $k$ -th photonic qubit in the ground state, i. e., in the state  $|0_k\rangle$  without a photon. In that case, the CNOT gate simply corresponds to a conditional emission gate from the matter qubit,

$$d_0 |D\rangle \otimes |0_k\rangle + g_0 |G\rangle \otimes |0_k\rangle \rightarrow d_0 e^{-i\omega_0 T_p} |D\rangle \otimes |0_k\rangle + g_0 |G\rangle \otimes |1_k\rangle, \quad (\text{S28})$$

where  $|1_k\rangle$  denotes the state with one photon in the  $k$ -th time bin and  $T_p$  is the gate duration. This operation can be engineered in three simple steps. First, the amplitude in the ground state is transferred to the single-excitation dark state  $|A\rangle$  by applying  $\mathcal{R}_{GA}(\pi/2, 0, 2J_{GA}T_{GA})$ , which results in the state  $d_0 e^{-2iJ_{GA}T_{GA}} e^{-i\omega_0 T_{GA}} |D\rangle \otimes |0_k\rangle - ig_0 e^{-i\omega_0 T_{GA}} |A\rangle \otimes |0_k\rangle$  after a gate time  $T_{GA}$  and under a constant coherent exchange interaction  $J_{GA}$ . Second, a detuning is applied to the second emitter only, which couples  $|B\rangle$  to  $|A\rangle$  (but not to  $|D\rangle$ ) and thereby generates a conditional photon of duration  $T_{em}$ . The resulting state reads,  $d_0 e^{i\xi} e^{-i\omega_0(T_{GA}+T_{em})} |D\rangle \otimes |0_k\rangle + g_0 |G\rangle \otimes |1_k\rangle$ . Here, we have defined the phase  $\xi = -2J_{GA}T_{GA} + 4 \int_0^{T_{em}} J(t') dt'$ , where  $J(t)$  is the sequence applied during the emission process to obtain a target photon wavepacket  $\psi_{ph}(t)$ . Finally, performing the phase gate  $\mathcal{P}_D(\xi)$  by applying a constant detuning  $\Delta$  over a time  $T_D = \xi/|\Delta|$  corrects the additional phase acquired by  $|D\rangle$  and completes the CNOT gate in Eq. (S28) with  $T_p = T_{GA} + T_{em} + T_D$ .

### III.B. CZ gate

To apply a controlled phase gate on the photonic qubit emitted at step  $k$ , the photonic qubit is reflected by a switchable mirror placed at the transmitting end of the half-waveguide [S28]. The subsequent scattering with the collective system allows to engineer a CZ gate that only performs a sign flip to the state  $|G\rangle \otimes |1_k\rangle$ . We assume that the bandwidth (or inverse duration) of the photon is much smaller than the decay rate of the collective bright state, such that the emitters are weakly driven. In this regime, the phase  $r$  picked by the incoming photon upon reflection from the switchable mirror and the collective system is [S51]

$$r = 1 - i \frac{3\gamma_0}{\Omega_B} \langle \hat{\sigma}_B \rangle, \quad (\text{S29})$$

where  $\Omega_B$  is the small Rabi frequency associated to the incoming photon, and  $\hat{\sigma}_B = \hat{S} = (\hat{\sigma}_1 + \hat{\sigma}_2 + \hat{\sigma}_3)/\sqrt{3}$  corresponds to the jump operator of the collective system into the waveguide.

Let us first study the case where the matter qubit is initially in the ground state  $|G\rangle$  and the incoming photon weakly excites the single-excitation bright state  $|B\rangle$ . For  $\delta = -J$  (such that the single-excitation dark states remain eigenstates of the Hamiltonian interaction) and for weak drive with frequency  $\omega_L = \omega_0$  and strength  $\Omega \ll |\Delta + J - i3\gamma_0/2|$ , the amplitudes in the states  $|G\rangle$  and  $|B\rangle$  are

$$\dot{g}(t) = -i\Omega b(t), \quad (\text{S30a})$$

$$\dot{b}(t) = -i(\Delta + J - i\frac{3\gamma_0}{2}) - i\Omega g(t). \quad (\text{S30b})$$

Due to the weak drive, the single-excitation bright state can be adiabatically eliminated. To leading order in the small parameter  $|\Omega/(\Delta + J - i3\gamma_0/2)|$ , the amplitude in the ground state remains  $g(t) \approx 1$ , while the amplitude in  $|B\rangle$  reads  $b(t) \approx -\Omega/(\Delta + J - i3\gamma_0/2)$ . Noting that  $\langle \hat{\sigma}_B \rangle = b$ , we readily find the reflection coefficient for the ground state

$$r_G = 1 - 2 \frac{3\gamma_0}{3\gamma_0 + 2i(J + \Delta)}. \quad (\text{S31})$$

Similarly, the photon couples the single-excitation dark state  $|D\rangle$  to the two-excitation bright state  $|S_D\rangle$ . Following an analogous derivation for the matter qubit initially in  $|D\rangle$ , we find the reflection coefficient

$$r_D = 1 - 2 \frac{\gamma_0}{\gamma_0 + 2i(\Delta - J)}. \quad (\text{S32})$$

As expected, the reflection coefficients  $r_G$  and  $r_D$  are respectively dictated by the decay rates of the collective states  $|B\rangle$  and  $|S_D\rangle$  and the off-resonance of the corresponding transitions. Note that the effect of the two mirrors (i. e.,

the mirror forming the half-waveguide and the switchable mirror to reflect the photonic qubits back to the collective system) cancels out, such that a resonant photon acquires a phase flip ( $r = -1$ ) whereas a far off-resonant one does not ( $r = 1$ ).

The CZ gate is obtained by driving on resonance with the  $|G\rangle \leftrightarrow |B\rangle$  transition, i.e., for  $\Delta = -J$ . In that case,  $r_g = -1$  and the photon acquires a phase flip when scattering of  $|G\rangle$ . When the matter qubit is in  $|D\rangle$ , however, the reflection coefficient  $r_d = -e^{i\phi}$  is given by the phase  $\phi = 2 \arctan(4J/\gamma_0)$ , which approaches  $r_d \rightarrow 1$  for  $J \gg \gamma_0$ . The resulting ideal gate for the  $k$ -th photon reads

$$\text{CZ}(J) = |G\rangle \langle G| \otimes (|0_k\rangle \langle 0_k| - |1_k\rangle \langle 1_k|) + |D\rangle \langle D| \otimes (|0_k\rangle \langle 0_k| + e^{2i \arctan(4J/\gamma_0)} |1_k\rangle \langle 1_k|), \quad (\text{S33})$$

which implements the CZ gate in the limit  $J \gg \gamma_0$ .

Due to the finite bandwidth of the photons (i.e., their frequency distribution around  $\Delta = -J$ ), the scattered wavepacket from  $|G\rangle$ ,  $\tilde{\psi}_{\text{ph}}^{(G)}(t)$ , and  $|D\rangle$ ,  $\tilde{\psi}_{\text{ph}}^{(D)}(t)$ , are not identical to the incoming wavepacket,  $\psi_{\text{ph}}(t)$ . By means of the Fourier decomposition of the incoming wavepacket,

$$\Psi_{\text{ph}}(\omega) = \frac{1}{\sqrt{2\pi}} \int_{-\infty}^{\infty} d\omega \psi_{\text{ph}}(t) e^{i\omega t}, \quad (\text{S34})$$

we readily compute the scattered wavepacket as

$$\tilde{\psi}_{\text{ph}}^{(\lambda)}(t) = \frac{1}{\sqrt{2\pi}} \int_{-\infty}^{\infty} d\omega \Psi_{\text{ph}}(\omega) r_{\lambda}(\omega) e^{-i\omega t}, \quad (\text{S35})$$

where  $\lambda \in \{G, D\}$  represents the scattering process from each collective state. The frequency-dependent reflection coefficients for  $|G\rangle$  and  $|D\rangle$  are obtained from Eq. (S31) and (S32) by substituting  $\Delta \rightarrow \omega - J$ . That is, given an incoming wavepacket  $\psi_{\text{ph}}(t)$ , the collective system performs the quantum operation

$$\tilde{U} = |G\rangle \langle G| \otimes (|0_k\rangle \langle 0_k| + |1_k, \tilde{\psi}_{\text{ph}}^{(G)}\rangle \langle 1_k, \psi_{\text{ph}}|) + |D\rangle \langle D| \otimes (|0_k\rangle \langle 0_k| + |1_k, \tilde{\psi}_{\text{ph}}^{(D)}\rangle \langle 1_k, \psi_{\text{ph}}|). \quad (\text{S36})$$

The average gate fidelity can be computed as [S66–S68]

$$\mathcal{F} = \frac{1 + d^{-1} |\text{tr}(U^\dagger \tilde{U})|^2}{d + 1}, \quad (\text{S37})$$

where  $d = 4$  describes the dimension of the Hilbert space and  $U$  implements the perfect CZ gate,

$$U = |G\rangle \langle G| \otimes (|0_k\rangle \langle 0_k| - |1_k, \psi_{\text{ph}}\rangle \langle 1_k, \psi_{\text{ph}}|) + |D\rangle \langle D| \otimes (|0_k\rangle \langle 0_k| + |1_k, \psi_{\text{ph}}\rangle \langle 1_k, \psi_{\text{ph}}|). \quad (\text{S38})$$

Defining the overlap between the incoming and scattered wavepackets as

$$O_{\lambda} = \int_{-\infty}^{\infty} dt \psi_{\text{ph}}^*(t) \tilde{\psi}_{\text{ph}}^{(\lambda)}(t), \quad (\text{S39})$$

the average fidelity reads

$$\mathcal{F} = \frac{1}{5} + \frac{1}{20} |2 - O_G + O_D|^2. \quad (\text{S40})$$

(a) For the Gaussian wavepacket given by Eq. (S25), obtained by dynamically controlling the coupling between the auxiliary dark state  $|A\rangle$  and the bright state  $|B\rangle$  during the emission process, the overlaps are

$$O_G = 1 - \sqrt{\pi} 3\gamma_0 \tau e^{(3\gamma_0 \tau/2)^2} \left( 1 - \text{erf} \left( \frac{3\gamma_0 \tau}{2} \right) \right), \quad (\text{S41a})$$

$$O_D = 1 - \sqrt{\pi} \gamma_0 \tau e^{\tau^2 (\gamma_0 - 4iJ)^2/4} \left( 1 - \text{erf} \left( \tau \frac{\gamma_0 - 4iJ}{2} \right) \right). \quad (\text{S41b})$$

Large overlaps are obtained when the duration  $\sim \tau$  of the wavepacket is much larger than the lifetime of the bright states  $\sim \gamma_0^{-1}$ , such that the photon effectively acts as a weak drive. This corresponds to the limit where the bandwidth

of the photon,  $\mathcal{B} = \tau^{-1}$ , is much narrower than the bright state decay rates, that is,  $\mathcal{B}/\gamma_0 \ll 1$ . Then, the average gate fidelity reads

$$\mathcal{F} = 1 - \frac{4}{5} \frac{\gamma_0^2}{\gamma_0^2 + 16J^2} - \frac{8}{45} \frac{\mathcal{B}^2}{\gamma_0^2} + \mathcal{O}\left(\frac{\mathcal{B}^4}{\gamma_0^4}\right) + \mathcal{O}\left(\frac{\mathcal{B}^2 \gamma_0^3}{\gamma_0^2 J^3}\right). \quad (\text{S42})$$

The first error term arises from the phase  $\phi = 2 \arctan(4J/\gamma_0) \neq \pi$  at finite  $J/\gamma_0$ . The second error term arises from the finite bandwidth of the photon scattering from  $|G\rangle$ . Note that the error associated to the finite bandwidth of the photon scattering from  $|D\rangle$  is suppressed by an additional factor  $\gamma_0^3/J^3$ .

(b) For the photon wavepacket given by Eq. (S22) under the substitution  $J \rightarrow \tilde{J}$ , obtained by applying a constant coupling  $\tilde{J} < \gamma_0/\sqrt{32}$  during the emission process, the overlaps are found to be

$$O_G = -\frac{\gamma_0^2 - 4\tilde{J}^2}{\gamma_0^2 + 4\tilde{J}^2}, \quad (\text{S43a})$$

$$O_D = -\frac{(\gamma_0 + 4iJ)(\gamma_0 - iJ) - 18\tilde{J}^2}{(\gamma_0 - 4iJ)(\gamma_0 - iJ) + 18\tilde{J}^2}. \quad (\text{S43b})$$

In this case, the photon wavepacket is asymmetric. It is centered around  $t_{\text{av}} = \int_{-\infty}^{\infty} |\psi_{\text{ph}}(t)|^2 t dt = 2/(3\gamma_0) + \gamma_0/(24\tilde{J}^2)$  and has a temporal width  $\tau^2 = \int_{-\infty}^{\infty} |\psi_{\text{ph}}(t)|^2 (t - t_{\text{av}})^2 dt \approx 5\gamma_0^2/(576\tilde{J}^4)$ . The overlap is maximal for large temporal widths  $\tau$ , and therefore for small values of  $\tilde{J} \ll \gamma_0$ . In this limit, the fidelity of the CNOT gate reads

$$\mathcal{F} = 1 - \frac{4}{5} \frac{\gamma_0^2}{\gamma_0^2 + 16\tilde{J}^2} - \frac{16}{5} \frac{\tilde{J}^2}{\gamma_0^2} + \mathcal{O}\left(\frac{\tilde{J}^4}{\gamma_0^4}\right) + \mathcal{O}\left(\frac{\tilde{J}^2 \gamma_0^3}{\gamma_0^2 \tilde{J}^3}\right). \quad (\text{S44})$$

The error scales linearly with the bandwidth  $\mathcal{B} = \tau^{-1}$  of the photon,  $\tilde{J}^2/\gamma_0^2 \propto \tau^{-1}\gamma_0^{-1} \propto \mathcal{B}\gamma_0^{-1}$  (faster than for the case of a Gaussian photon).

#### IV. PHOTONIC ENTANGLED STATE GENERATION WITH TWO TWO-LEVEL EMITTERS COUPLED TO A HALF-WAVEGUIDE

The CNOT or conditional emission gate for a collective system composed of three two-level emitters relies on the existence of the auxiliary dark state  $|A\rangle$ , whose coupling to the bright state  $|B\rangle$  can be controlled over time (see Section III of the Supplemental Material). This provides two main advantages. First, it allows to emit a single photon using only classical driving fields, such that the states of photonic qubit correspond to zero or one photon exactly. Second, it allows for an efficient and simple control of the wavepacket of the photonic qubit.

Photonic entangled state generation is also possible with just two two-level emitters coupled to the half-waveguide at distances  $x_n = (n + 1/4)\lambda_0$  from the mirror. The decoherence-free subspace is now formed by two states, the ground state  $|G\rangle \equiv |gg\rangle$  and the single-excitation dark state  $|D\rangle \equiv (|eg\rangle - |ge\rangle)/\sqrt{2}$ , which also form the matter qubit. The remaining two states,  $|B\rangle \equiv (|eg\rangle + |ge\rangle)/\sqrt{2}$  and  $|E\rangle \equiv |ee\rangle$  are bright and decay at a rate  $2\gamma_0$ . Again, arbitrary rotations within the decoherence-free subspace are obtained via a weak classical field of the form  $\hat{H}_{\Omega,D} = \Omega(\hat{\sigma}_1 - \hat{\sigma}_2)/\sqrt{2} + h.c.$ , such that population of bright states is prevented by the Zeno effect ( $\Omega \ll \gamma_0$ ) and the photon blockade (for large coherent exchange interactions  $J \gg \Omega_0$  between emitters).

Due to the absence of an auxiliary dark state, the CNOT gate needs to be performed by rapidly transferring the amplitude in  $|G\rangle$  to a bright state via the drive  $\hat{H}_{\Omega,B} = \Omega(\hat{\sigma}_1 + \hat{\sigma}_2)/\sqrt{2} + h.c.$  in a time  $T \ll \gamma_0^{-1}$  (such that no photon emission occurs during the transfer). In the absence of a coherent exchange interaction  $J$  between the emitters,  $|G\rangle \leftrightarrow |B\rangle \leftrightarrow |E\rangle$  are resonantly coupled, and only the doubly-excited state  $|E\rangle$  can be prepared after a time  $T = \pi/\sqrt{2}\Omega$ . As a result, the two states of the photonic qubit correspond to zero and two photons. Generation of photonic qubits encoded as zero and one photons requires a non-linearity that allows the transfer  $|G\rangle \rightarrow |B\rangle$  while suppressing the coupling between  $|B\rangle$  and  $|E\rangle$ . For superconducting qubits, this can be achieved by applying  $\hat{H}_{\Omega,B}$  for a time  $T = \pi/2\Omega$  under a large coherent interaction  $J \gg \Omega \gg \gamma_0$  that renders both transitions off-resonant by  $2J$ . For neutral atoms coupled to waveguides, the non-linearity can be attained via Rydberg interactions if both atoms are within a Rydberg blockade radius. Additionally, control of the wavepacket of the emitted photons requires a tunable coupling strength  $\gamma_0$  of the emitters to the waveguide over time [S28]. This stays in stark contrast to the

three-emitter setup, where the auxiliary dark state allows to control the wavepacket by simply varying the detuning of one emitter over time.

Finally, the controlled phase gate or CZ gate can be easily achieved in the case of two emitters coupled to a waveguide. The reflection coefficient for an incoming photon in the low intensity limit reads  $r = 1 - 2i\gamma_0\langle\hat{S}\rangle/\Omega$ . Since the single-excitation dark state  $|D\rangle$  ( $\langle\hat{S}\rangle = 0$ ), leading to  $r_d = 1$ . If the emitter system is in  $|G\rangle$ , however, the amplitude in the bright state in the low intensity limit is  $b(t) \approx -\Omega/(\Delta - i\gamma_0)$ . Noting that  $\langle\hat{S}\rangle = b$ , we obtain the reflection coefficient for the ground state  $r_g = 1 - 2\gamma_0/(\gamma_0 + i\Delta)$ . Thus, the scattered photon acquires a phase flip ( $r_g = -1$ ) if it is on resonance with the  $|G\rangle \leftrightarrow |B\rangle$  transition ( $\Delta = 0$ ), thereby implementing the CZ gate given in Eq. (S38).